

## Amelioration of Dextran Sulfate Sodium-induced Chronic Colitis by Sulfasalazine Salicylazosulfapyridine *via* Reducing NF- $\kappa$ B Transcription Factor p65 Recruitment to ICAM-1 Gene Promoters

Wenchang ZHAO,<sup>a</sup> Lijun SONG,<sup>\*,b</sup> and Deng HONGZHU<sup>c</sup>

<sup>a</sup>School of Pharmacy, <sup>b</sup>Institute of New Drug Development, Guangdong Medical College, Dongguan, Guangdong, 523808, PR China, and <sup>c</sup>School of Traditional Chinese Medicine, Southern Medical University, Guangzhou, Guangdong, 510515, PR China

(Received March 29, 2010; Accepted May 18, 2010)

Sulfasalazine salicylazosulfapyridine (SASP), consisting of 5-aminosalicylic acid bound to sulfapyridine by a diazo bond, is an effective drug in the treatment of inflammatory bowel diseases (IBD). However, its mechanism of action remains a matter of debate. The objective of our work was to investigate SASP's effect on NF- $\kappa$ B signal transduction pathway in transcriptional regulation level. Repeated colitis was induced by administration of 4 cycles of 4% dextran sulfate sodium (DSS); The severity of colitis was assessed on the basis of clinical signs, colon length, and histology scores. Moreover, sIgA and haptoglobin (HP) were analyzed by enzyme linked immunosorbent assay, and ICAM-1 gene expression was analyzed by quantitative reverse transcriptase real-time polymerase chain reaction (qRT-PCR) using SYBA green I. NF- $\kappa$ B signal transduction proteins and transcriptional factor p65 interaction with promoter of ICAM-1 were assessed by western blotting and chromatin immunoprecipitation assay. SASP administration significantly attenuated the colitis signs and caused substantial reductions of HP expression, and maintained the level of cecum sIgA. SASP inhibited ICAM-1 gene expression and had no effect on MIF gene expression. Also, SASP was able to reduce p-I $\kappa$ B $\alpha$  protein expression; however, no change in the activation of IKK $\alpha$ , IKK $\beta$ , p65, and I $\kappa$ B $\alpha$  was noted. SASP inhibited p65 recruitment to the gene ICAM-1 promoter. In conclusion, inhibition of NF- $\kappa$ B pathway signal proteins and blockade of p65 binding to gene ICAM-1 promoter might explain the effect and mechanisms of SASP at alleviating DSS-induced colitis in mice.

**Key words**—sulfasalazine salicylazosulfapyridine; dextran sulfate sodium; NF- $\kappa$ B; ICAM-1; colitis

### INTRODUCTION

Sulfasalazine salicylazosulfapyridine (SASP), the prodrug of 5-ASA, is an effective treatment against inflammatory bowel diseases (IBD) by blocking the production of prostaglandins and leukotrienes, inhibiting bacterial peptide induced neutrophil chemotaxis and adenosine-induced secretion, scavenging reactive oxygen metabolites and so on.<sup>1–4)</sup> Although this drug has been used for decades, its mechanism of action remains a matter of debate.

IBD comprises a number of the chronic immunoinflammatory disorders of the gastrointestinal tract in which this immunological balance is severely impaired.<sup>5–7)</sup> The nuclear transcription factor kappaB (NF- $\kappa$ B) has been identified as one of the key regulators in this immunological setting. The amount of activated NF- $\kappa$ B correlated significantly with the severity of intestinal inflammation.<sup>8,9)</sup> Accumulating evi-

dence has indicated that migration of leucocytes to the site of inflammation is related to ICAM-1, and enhanced colonic mucosal endothelial cell ICAM-1 expression is an early event in the inflammatory cascade of acute colitis.<sup>10,11)</sup> Proinflammatory factor ICAM-1 expression is regulated *via* NF- $\kappa$ B signal transduction activation. So far, there is no report about its effect on transcriptional regulation of the interaction of transcription factor p65 and promoter of gene ICAM-1 in ulcerative colitis.

The objectives of this study were therefore to examine the effects and potential mechanisms of SASP on chronic colitis. To address these objectives, we employed repeated colitis model in C57bl/6 mice induced by administration of 4 cycles of 4% dextran sulfate sodium (DSS), which produces inflammation limited to the colonic mucosa that is closely related to human ulcerative colitis.<sup>12,13)</sup>

### METHODS

**Materials** SASP was purchased from Shanghai

\*e-mail: songlijun6981@126.com

Fuda pharmaceutical company (Shanghai, China). DSS (molecular weight 5000) was obtained from Amersham Biosciences (Amersham Biosciences Pharmacia Biotech, Sweden); Hematoxylin and eosin stain was purchased from Sigma Chemical Co. (St Louis, MO); RNAlate Solution was from Ambion, total RNA extract reagent was purchased from Invitrogen and SYBR Prime Script™ RT-PCR kit was purchased from TAKARA Biotechnology (Dalin, China). Whole cell extraction kit was obtained from Chemicon International. PhosSTOP Phosphatase Inhibitor Cocktail Tablet was purchased from Roche Diagnostics GmbH Applied Science. BCA Protein Assay Kit was purchased from Pierce Co.; NF- $\kappa$ B Pathway Sampler Kit containing IKK $\alpha$  antibody, IKK $\beta$  (L570) antibody, NF- $\kappa$ B p65 rabbit mAb, I $\kappa$ B $\alpha$  mouse mAb (amino-terminal antigen), phospho-I $\kappa$ B- $\alpha$ (Ser32) rabbit mAb, anti-rabbit IgG, HRP-linked antibody, and anti-mouse IgG was purchased from Cell Signaling Technology, Inc. Anti rabbit PVA-6001 IgG-HRP was from Beijing Zhongshan. EZ-ChIP Chromatin Immunoprecipitation Kit was from Millipore Corporation. Enzyme linked immunosorbent assay sIgA and HP Kit were purchased from Nanjing Jianchen Bioscientific. All other reagents were analytical grade.

**Animal Care** Female C57BL/6 mice, 6 weeks of age, obtained from the animal centre of Southern Medical University were housed 5–6/cage, and kept at the animal house facilities with room temperature of  $20 \pm 2^\circ\text{C}$ , 50% humidity and 12: 12-h light-dark cycles, fed a standard pellet diet, and administered tap water *ad libitum*. The Animal Research Board Committee of Southern Medical University approved the studies. Mice were acclimatized for 2 weeks before the study. Body weights, drink water and food consumption were measured every week for the duration of the experiment.

After a 7-day acclimation period, a total of 36 mice were randomly distributed into three groups. Group 1 ( $n=11$ ) was administered water as normal control. Groups 2 and 3 received four cycles of DSS administration (each cycle 4% DSS dissolved in distilled water for 7 days then distilled water alone for 7 days). This schedule was used to simulate the cycle of acute flare-ups alternating with periods of disease inactivity observed in human ulcerative colitis patients.<sup>13,14</sup> Group 2 ( $n=15$ ) was administered distilled water by oral gavage 10 ml/kg once daily for the whole ex-

perimental period. Group 3 ( $n=10$ ) was administered SASP 4 g/10 ml/kg solution by oral gavage once daily for the whole experimental period. Mice were weighed every week for the determination of percent weight change. This was calculated as: % weight change = (weight at week X - weight at week 0)  $\times$  100. Animals were monitored clinically for occult and rectal bleeding, diarrhea, and general signs daily. Occult blood in the feces was evaluated by the orthotolidine methods. Occult blood scores and stool consistency scores were determined according to a standard scoring system, as previously described by Shimon *et al.*<sup>14</sup>

**Histological Scoring** The mice were killed by dislocation after 56 days' experiments. The colon was resected between the ileocecal junction and the proximal rectum, close to its passage under the pelvisternum. The colon was placed onto a non-absorbent surface and measured by a ruler, taking care not to stretch the tissue. Colon length was measured as an indication of colonic inflammation. Some colonic tissues were stored at  $-80^\circ\text{C}$  for PCR and western blotting.

The colonic tissues were fixed with 10% neutral buffered formalin. Serial tissue sections (3  $\mu\text{m}$ ) were made and mounted on glass slides and routinely stained with hematoxylin and eosin and Alcian blue for histopathological analysis. Sections were coded with an accession number and reviewed by a pathologist without access to the code. Each section was scored for lesions based on severity, ulceration, hyperplasia and crypts alteration according to the method of Melgar *et al.*<sup>13</sup>

**Scanning Electron Microscopy** Specimens from all groups were processed using a standard technique for scanning electron microscopy (SEM). Fragments 4 mm from colonic tissues were fixed with 2.5 glutaraldehyde in 0.1 M Sorensen's phosphate buffer (pH7.4) at room temperature for 24 h. Samples were then postfixed in a phosphate-buffered 2% osmium tetroxide solution at  $4^\circ\text{C}$  for 1 h. The samples were glued onto stubs, coated with gold in a SCD040 Balzer Sputterer and observed by a Philips 505 SEM at 10–30 kV.

**Immunohistochemistry** Immunohistochemical staining was performed by avidin-biotin peroxidase complex method as described previously.<sup>16</sup> In brief, endogenous peroxidase activity was quenched in paraffin-embedded tissue sections with 1%  $\text{H}_2\text{O}_2$ . An-

tigen was retrieved by pretreatment with citrate buffer in high pressure heating then the slides were incubated with primary antibody ICAM-1 (1: 1000 dilution) followed by the appropriate PV-6001 IgG secondary antibody for 45 min each. Diaminobenzidine was used as chromagen. Slides were washed thoroughly between incubations with PBS. Negative controls were established by replacing the primary antibody with PBS and normal serum. Positive staining was indicated by the presence of brown-colored precipitate.

#### **Production of Secretory Immunoglobulin A**

Cecum content was collected rapidly, suspended in twofold saline (V/W), and centrifuged at 5000rpm and 4°C for 5 min. Content of cecum sIgA was determined by mouse secretory immunoglobulin A (sIgA) double antibody sandwich ELISA Kit according to the manufacturer's protocol.

**Production of HP** Blood was collected into heparin tube from mice *via* removing eyeball. Care was taken to minimize hemolysis, and sample were stored at -20 °C. The HP concentrations in the plasma were determined similarly as sIgA.

**RNA isolation and qRT-PCR Using SYBR Green I Fluorescent Dye** Specimens were immediately stored in RNAlater solution for 24 h, then stored at -20°C. The RNAlater-preserved colon tissues were homogenized and extracted using trizol reagent according to the manufacturer's instructions. Extracted RNA was dissolved in 20  $\mu$ l water. Two  $\mu$ g of total RNA from each sample was converted into cDNA. cDNA synthesis was performed as kit instruction. Relative gene expression quantitation for ICAM-1, Macrophage-migration inhibitory factor (MIF) with GAPDH as internal reference gene, was carried out using MX3005 real time PCR amplification detection system in triplicate, based on the SYBR-Green method. Primer sequences were as follows: ICAM-1, sense 5'-CAACTGGAAGCTGTTTGAGCTGAG-3' and reverse 5'-AGGGTGAGGTCCTTGCCTACTTG-3'; MIF, sense 5'-CTGCACAGCATCGGCAAGA-3' and reverse 5'-TTGGCAGCGTTCATGTCGTAA-3'; GAPDH, sense 5'-AAATGGTGAAGTCCGGTGTG-3' and reverse 5'-TGAAGGGGTCGTTGATGG-3'. The PCR reaction mixture consisted of 0.1  $\mu$ mol/l of each primer, 1  $\times$  SYBR Premix EX Taq (Perfect Real Time) premix reagent, and 50 ng cDNA to a final volume of 20  $\mu$ l. Cycling conditions were 95°C for 10 min, followed by 40 cycles at premature 95°C for 5 s, annealing temperature was 59°C, 30 s. PCR specificity

was confirmed by dissociation curve analysis and gel electrophoresis. The relative induction of gene mRNA expression, comparative Delta-delta Ct was calculated using the following equation:  $\Delta\Delta Ct = (Ct, target-Ct, GAPDH)_{treatment} - (Ct, target-Ct, GAPDH)_{nontreatment}$ , and final data were derived from  $2^{-\text{average}\Delta\Delta Ct}$ . GAPDH was used as internal control.

**Western Blot Analysis** Colonic tissue was dounced on ice and lysed by adding protease inhibitor cocktail and PhosSTOP working solutions. Protein 100 mg was subjected to electrophoresis on 10% SDS-polyacrylamide gels. p65 rabbit mAb, I $\kappa$ B $\alpha$  mouse mAb and phospho-I $\kappa$ B $\alpha$  (Ser32) rabbit mAb were used to detect immunoreactive NF- $\kappa$ B p65 (1: 2000), I $\kappa$ B $\alpha$  (1: 2000) and pho-I $\kappa$ B $\alpha$  (1: 2000), respectively. The membranes were visualized with ECL Plus reagent and viewed by Kodak image station 4000 MM digital imaging system. The reactions were carried out in triplicate.

**Chromatin Immunoprecipitation Analysis** Chromatin immunoprecipitation (Chip) analysis was performed according to Chip kit instruction. Briefly, colon tissues were crushed carefully to obtain pieces as small as possible with liquid nitrogen, cellular proteins and DNA were crosslinked by adding formaldehyde to PBS to a final concentration of 0.1%. Tissues were completely resuspended with 10 ml Glycine-Stop-Fix solution and lysed with SDS buffer. Lysates were sonicated utilizing an American Ultrasonic Processor VG 130 and precleared with Chip blocked protein G agarose. Lysates were then incubated at 4°C with anti-p65 antibody, anti-RNA polymerase II (Upstate Biotechnologies), and IgG antibodies overnight. Complexes were precipitated and serially washed three times each with low salt, high salt, LiCl wash and TE buffer. Washed complexes were eluted with freshly prepared elution buffer, and reverse crosslinks of protein/DNA complexes to free DNA. Then DNA was purified by PCR purification column. Purified DNA was then amplified across the ICAM-1 promoter region utilizing the primers sense 5'-GGAC-CAGACATCTTCCTTCCTTT-3' and reverse 5'-TCACTTCCCTTCTCCCACTCAC-3'. The amplified product was detected by the presence of a SYBR green I fluorescent signal and calculated as described in section on qRT-PCR.

**Statistical Analysis** Data were analyzed by SPSS 13.0 statistical software and are expressed as the

mean  $\pm$  S.D. Body weights were compared with repeated measure variance analysis and one way-ANOVA. *p*-Values considered statistically significant at  $<0.05$ .

## RESULTS

Mice treated with DSS  $\geq 40$  mg/g body weight/day are shown in Fig 1a. No mice death during experiment. As shown in Fig. 1c, the percent weight change of DSS-induced colitis had obviously decreased and colitis gave rise to visible bloody stools, perianal bleeding, and weak strength. Inflammatory changes of the intestinal tract were associated with significant ( $p < 0.01$ ) augmentation of weight/length of the mice colon (Table 1). The colon for DSS-treated mice appeared edematous, and the intestine wall was thick and inflamed with fibrotic thickening of tissue while soft and amorphous as shown in Fig. 2.

Whereas SASP treatment in DSS-mice significantly reduced loss of body weight, stool consistency scores, and fecal occult blood score as shown in Fig. 1. No significant increase in the weight/length of the mice colon and spleen coefficient was found in SASP group compared with normal group ( $p > 0.05$ ).

On histological examination of colon from normal group mice, the histological features of the colon were typical of a normal structure. In DSS-treated mice, the inflammation extended through the mucosa, muscularis mucosae and submucosa. Extensive granulation tissue with the presence of fibroblasts and lymphocytes, leukocytes, and diffuse inflammatory infiltrates was apparent. In some sections of ulcerated areas necrotic tissue adjacent to surface cells could be observed. The mucosa adjacent to ulcers showed grossly elongated crypts. Furthermore, severe and extensive denudation of the surface epithelium (erosions) and mucodepletion of glands appeared. After

administration of SASP, the colonic histopathology was dramatically reduced, there was attenuation of morphological signs of cell damage, the colonic mucosa showed ulcers in the process of healing, evolution to a more chronic inflammatory infiltrate, with mononuclear predominance and initiation of a repair process. Goblet cells with Alcian blue-positive cells (acid glucoproteins such as sialomucins) were clearly observed in regions with reepithelization of the mucosal layer, whereas in contrast, remarkable mucin depletion was observed in ulcerative areas (Fig. 3).

ICAM-1-immunohistochemistry showed strong immunoreactivity in the mucosa, muscularis mucosae and submucosa in DSS group, whereas in contrast, SASP reduced positive cell numbers and stain intensity. Quantitation of immunostain-positive cell numbers percentage showed that there was significant difference between normal and DSS group ( $8.84 \pm 0.54$  vs.  $95.21 \pm 1.54$ ). Stain intensity was also greater in DSS groups compared with SASP group, as shown in Fig. 4.

SEM observations of the colonic mucosa in normal group mice showed well-defined concave grooves, and regular-shaped crypt openings containing mucin-like material. Mice that underwent 4 cycles of DSS administration showed widened grooves, dilatations of glandular crypts losing their regular shape by assuming fissure-like aspects, petal-like swelling and depletion of goblet cells, leaving an irregular crater-like area. A widely damaged surface epithelium with a dis-homogeneous distribution of microvilli characterized the inflamed mucosa (Fig. 5). Whereas SASP group showed integrity of mucosa architecture, with filamentous microvilli, surface loosening and no swelling.

As show in Fig. 6, an important increase in plasma HP and decrease in cecum sIgA characterized the colitis caused by DSS, which was consistent with the histological findings. Moreover, after treatment with SASP, the data clearly indicate a significant reverse alteration.

We then analyzed levels of gene ICAM-1 expression measured by qRT-PCR. The amplification kinetics of the gene ICAM-1, MIF and GAPDH assays were approximately equal and gel electrophoresis of PCR products was single band, therefore we used comparative Ct ( $\Delta\Delta Ct$ ) method for determination of ICAM-1 gene expression. As shown in Fig. 7, the ICAM-1 gene expression fold change of DSS treated

Table 1. Effect of SASP on Quantified Parameters of C57BL/6 Mice with Chronic Colitis Induced by 4 Cycles DSS Exposure

Groups	<i>n</i>	Histological grading	Spleen coefficient (g/g)	Ratio of colon weight and colon length (g/cm)
Normal	11	0.00 $\pm$ 0.000	0.0023 $\pm$ 0.00032	0.027 $\pm$ 0.0036
DSS	15	13.47 $\pm$ 0.834**	0.0089 $\pm$ 0.0032**	0.038 $\pm$ 0.0027**
SASP	10	8.00 $\pm$ 0.943▲▲	0.0038 $\pm$ 0.0009▲▲	0.026 $\pm$ 0.0024▲▲

Data are expressed as mean  $\pm$  S.D. \*\*  $p < 0.01$  vs. normal group; ▲▲  $p < 0.01$  vs. DSS group.

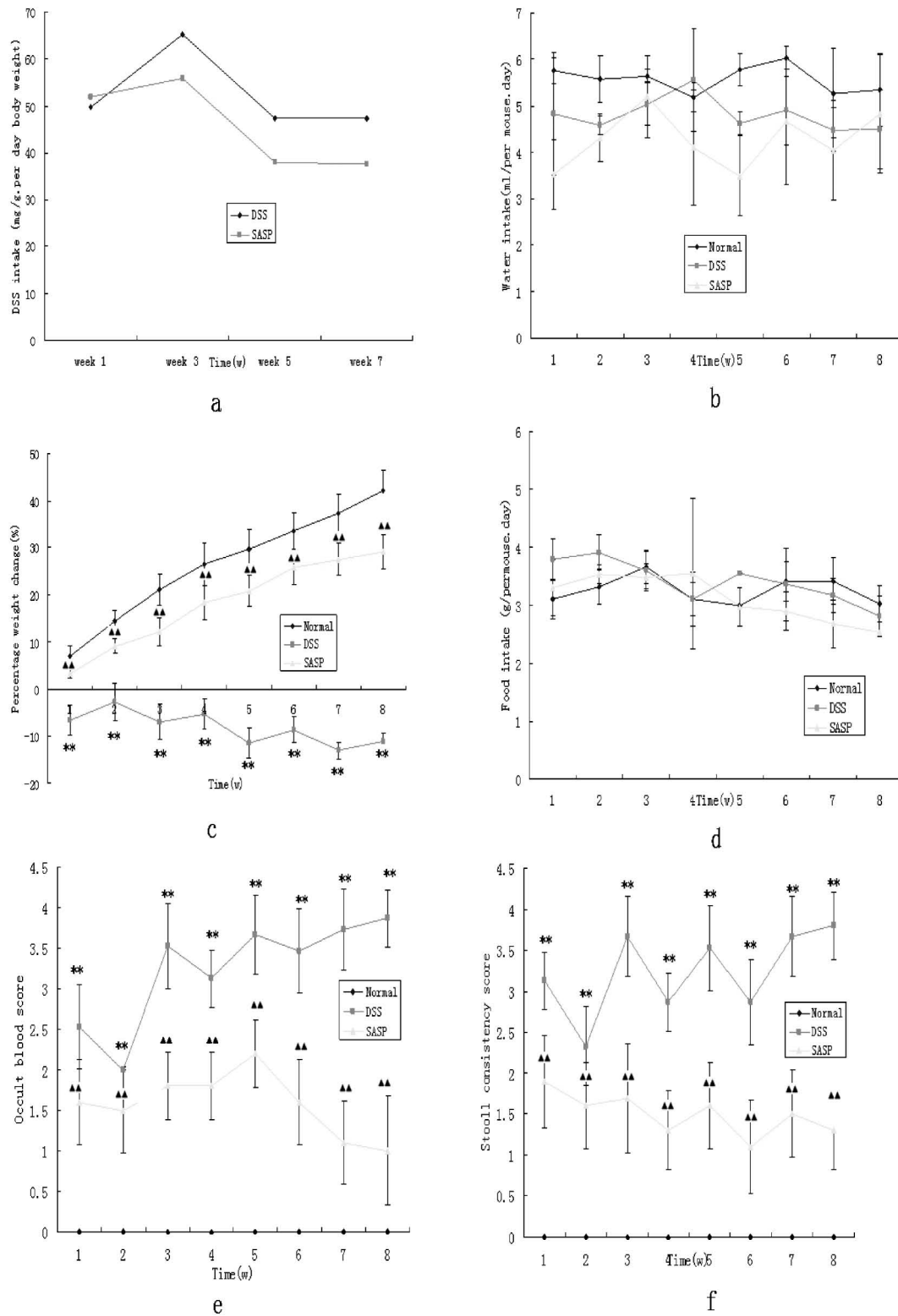


Fig. 1. Effect of SASP on DSS-induced C57BL/6 Mice Colitis

(a) DSS intake at different weeks. (b) Time-course of water intake. Weekly changes in water intake. (c) Time-course of percent body weight change. Weekly changes in body weight. Body weight change was calculated by (weight at week X - week0/weight at week0) × 100. (d) Time-course of food intake. Weekly changes in food intake. (e) Weekly changes in occult blood scores. (f) Weekly changes in stool consistency scores. Data are expressed as mean ± S.D. \*\**p* < 0.01 vs. normal ▲▲*p* < 0.01 vs. DSS control.

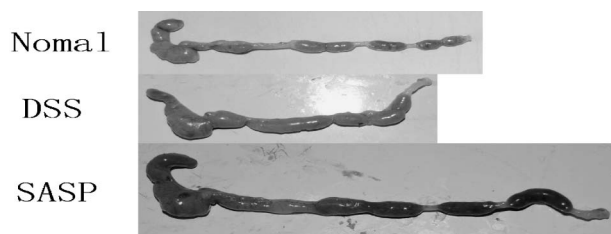


Fig. 2. Macroscopic View of the Large Bowel

mice was 2.60 vs. sham 0.32. Exposure of colon to DSS caused strong ICAM-1 expression, whereas on the contrary SASP induced downregulation of ICAM-1 expression in the treated groups *versus* DSS control. No significant change of gene MIF expression was observed.

DSS induced I $\kappa$ B $\alpha$  phosphorylation (0.63 vs. 0.30). Administration of SASP was able to diminish I $\kappa$ B $\alpha$  phosphorylation. However, no change in the activation of IKK $\alpha$ , IKK $\beta$ , p65 and I $\kappa$ B $\alpha$  was observed as shown in Fig. 8.

DSS treatment activated NF- $\kappa$ B transcriptional factor p65 binding at the ICAM-1 gene promoter, increasing to 6.47 vs. normal group 2.08 (Fig. 9). Conversely SASP reduced the NF- $\kappa$ B p65 binding at the ICAM-1 gene promoter. The SYBA green I PCR product of ICAM-1 promoter DNA fragmentation was validated by DNA sequencing.

## DISCUSSION

Clinically recommended drug therapies for IBD include 5-aminosalicylic acid, corticosteroids, immunosuppressants, immunoregulatory agents, antibiotics and probiotics, and anti-TNF- $\alpha$  therapy. The antiinflammation mechanism of corticosteroids for IBD is related to inhibition of PGs and release of proinflammatory cytokines, such as IL-1 and TNF- $\alpha$ . However in some patients, the side effects and steroid-resistant ulcerative colitis correlate with the dose and duration of corticosteroids treatment.<sup>17)</sup> Indeed, there is no clinically effective drug for IBD. SASP was first developed in 1942, this agent has been the parent aminosalicylate in use for >60 years and consists of 5-aminosalicylic acid linked by an azo bond to sulfapyridine. It combines an antibacterial agent (sulfapyridine) with an anti-inflammatory component (5-ASA).<sup>1)</sup> The sulfonamide moiety acts as a carrier to deliver the active component 5-ASA to the colon where it is released by bacterial action. SASP has

proven efficacy, and has a well-defined dose-response for induction of remission and maintenance of disease control in ulcerative colitis. The main mechanism includes inhibition of cyclooxygenase and lipoxygenase pathways to reduce production of PGs and leukotrienes, respectively.<sup>3)</sup> The principle findings of our study indicate that SASP could markedly improve symptom appearance after starting DSS administration. Average body weights in SASP group at the end of the experiment increased whereas DSS group showed obvious weight loss. There were no differences in average food and water consumption among all groups. As we know, the protective effect of mucus as an active barrier may be attributed largely to its viscous and gel-forming properties that are derived from mucin glycoprotein constituents. Alcian blue-positive cells seem to be associated with regenerative processes of the colonic mucosa, whereas by contrast, reduction of the cells is related to decreased resistance of the mucosa and paralleled by alterations in the normal pattern of maturation of mucin in goblet cells. sIgA is also a component of mucin, our experiment showed that SASP protected the crypt gland, mucous architecture, and maintained the cecum sIgA level. All these observations may have significance on the beneficial effect of SASP on colitis.

Compelling evidence suggested that increased luminal bacterial adherence is an important factor driving host colon mucosal immune system responses and contributes to an amplification loop of increased colonization and inflammation, and activates TLRs signaling pathways that culminates in activation of NF- $\kappa$ B transcription factors. Colon epithelia and local plasma cells produce preferentially secretory dimers and larger polymers of IgA and perform immune exclusion in first-line defense, thereby counteracting microbial colonization and mucosal penetration of soluble antigens.<sup>18,19)</sup> Plasma HP, one of the acute-phase proteins acts as the biological activity marker of inflammatory bowel disease, although none of the pertinent laboratory surrogate markers of disease activity in IBD is specific or sensitive enough to replace basic clinical observation such as the number of daily bowel movements, general well-being, and other parameters in parallel. SASP showed protective effect such as increase of cecum sIgA and decrease of plasma HP.

Accumulating evidence indicates that migration of leucocytes to the site of inflammation is related to

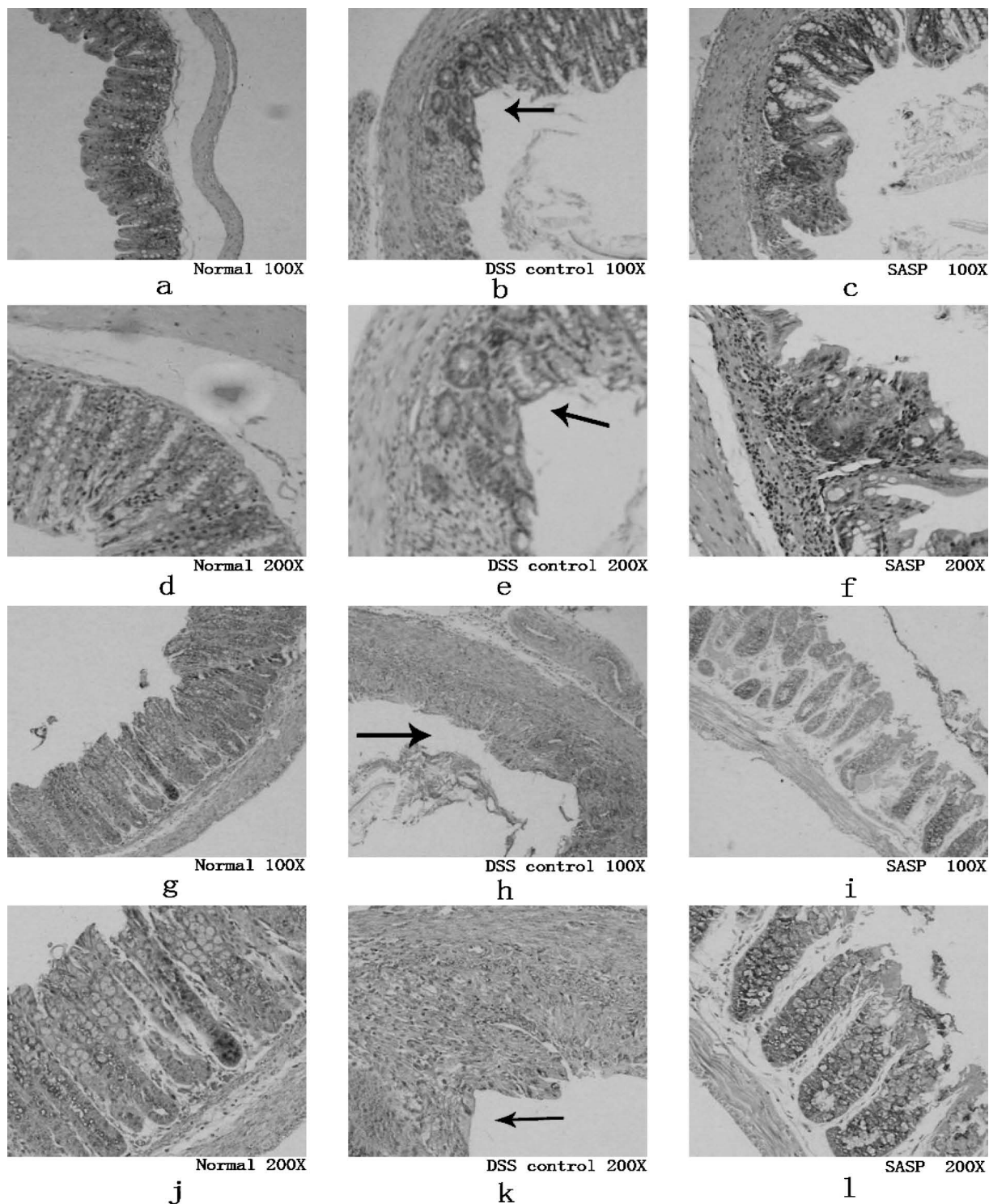


Fig. 3. Histological Sections of Colonic Mucosa from DSS Colitic Mice Stained with Haematoxylin and Eosin (a-f) and Alcian Blue (g-l)  
 (a, d, g and j) Noncolitic group showing normal histology of mice colon. (b, e, h and k) DSS control group showing extensive intestinal ulceration with severe inflammatory infiltrate in the lamina and submucosa, mucosa depletion (arrows). (c, f, i and l) SASP group showed attenuation of morphological signs of cell damage, and decrease of inflammatory cell infiltrate.

ICAM-1, and enhanced colonic mucosal endothelial cell ICAM-1 expression is an early event in the inflammatory cascade of acute colitis.<sup>10)</sup> Our results showed

that ICAM-1 gene expression was corrected with the development of colonic inflammation and moreover SASP administration was able to diminish ICAM-1

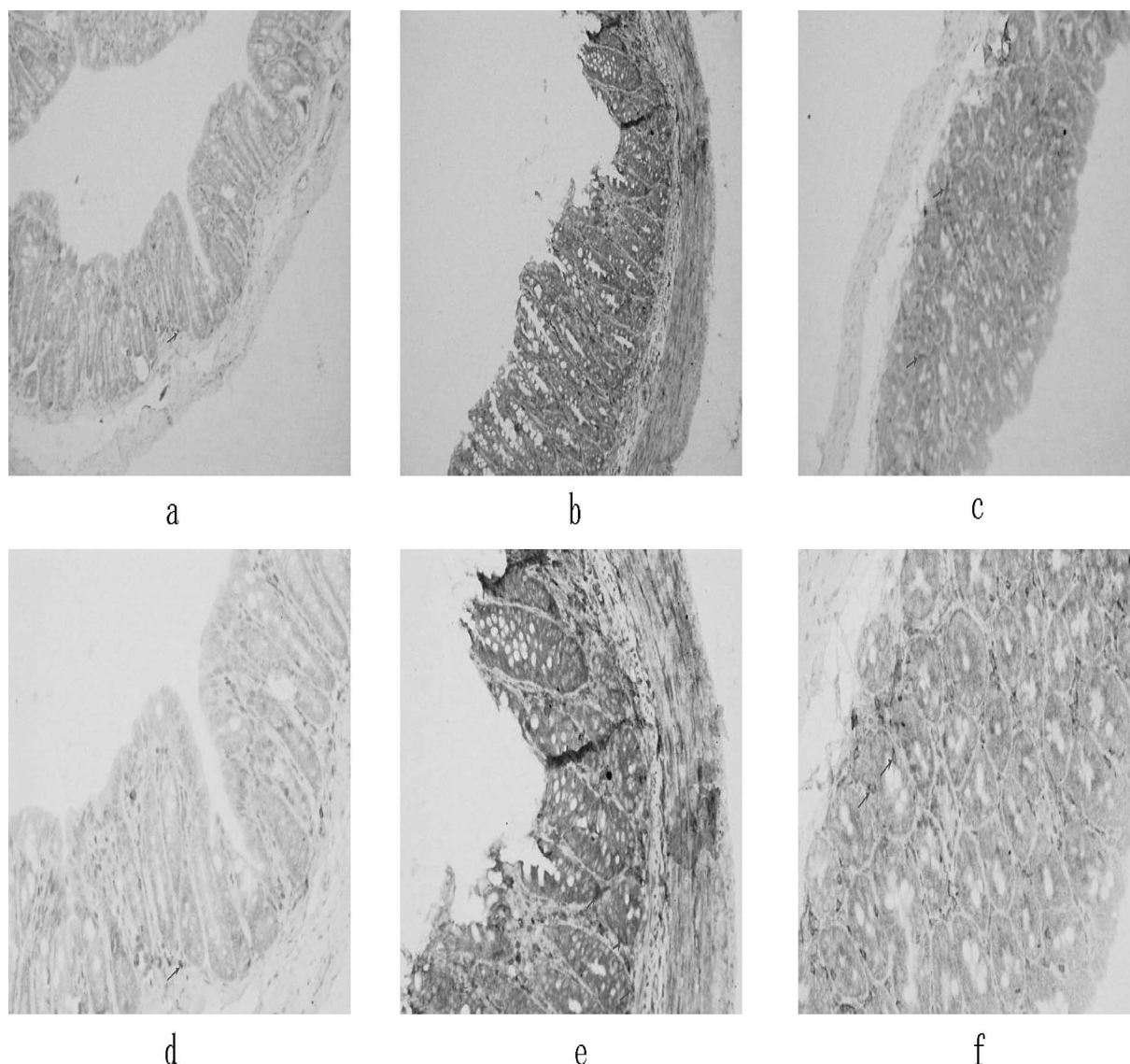


Fig. 4. Immunohistochemical Staining of the Colon Using Anti-ICAM-1 Monoclonal Antibody

a, d: Normal control mice. b, e: Mice with DSS colitis that had received distilled water demonstrated intense staining for ICAM-1 in epithelial cells and polynuclear infiltrates in the mucosa, muscularis mucosae, submucosa and the lamina propria. c, f: Section of colon from mice with DSS colitis that had received SASP after induction of colitis. Immunohistochemistry revealed that epithelial cell staining for ICAM-1 was considerably less intense than in mice that had received distilled water after induction of DSS colitis. Original magnification: a, b and c,  $\times 200$ . d, e and f,  $\times 400$ .

gene expression.

MIF is an ubiquitously expressed cytokine with a variety of mitogenic and pro-inflammatory functions.<sup>20-22</sup> Plasma concentrations of MIF in patients with active Crohn's disease were sixfold higher than in healthy individuals, and the development of chronic colitis is dependent on MIF.<sup>23</sup> Our data indicate that SASP had no apparent effect on MIF gene expression in DSS treated mice. Immune and inflammatory cytokines often activate NF- $\kappa$ B signal pathway, and induce p65 nucleus translocation for synthesis of numerous proinflammatory cytokines and adhesion

proteins such as ICAM-1.<sup>24,25</sup> Our results show that SASP administration induced I $\kappa$ B $\alpha$  phosphorylation.

At present, there are no data concerning the effect of SASP on transcriptional regulation on the interaction of transcription factor p65 and promoter of gene ICAM-1 in ulcerative colitis mice. Our research indicates that SASP inhibited the high level of TF p65 at the site of ICAM-1 promoter.

In summary, the data presented in the current study show that SASP reduces development of chronic experimental colitis and alleviates inflammatory response. We suggest that inhibition of NF- $\kappa$ B signal



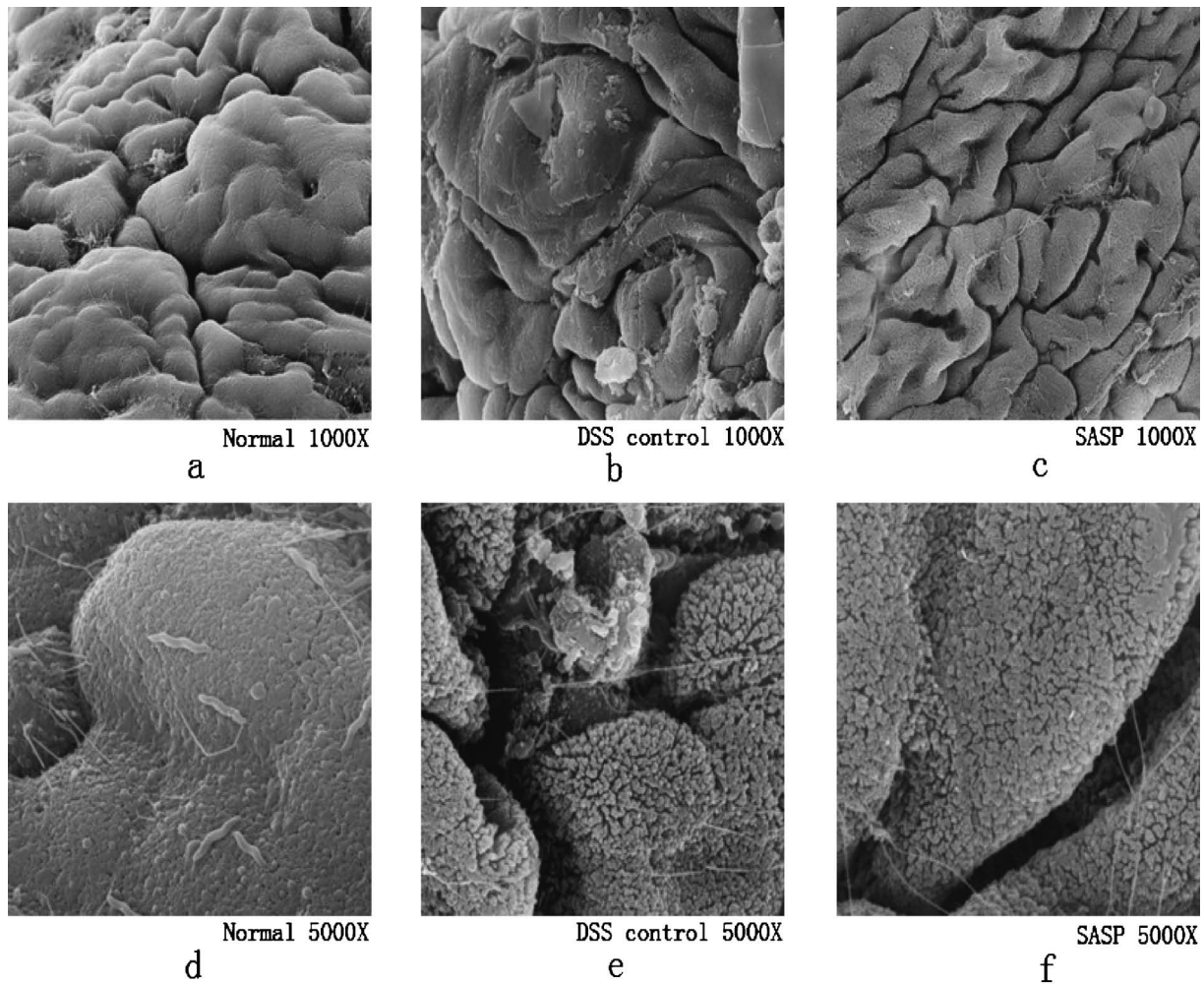


Fig. 5. SEM Observation

(a, d) Normal control mice showed normal aspect of the colonic mucosa. (b, e) Colonic mucosa of DSS mice: focal alteration of epithelial cells and slight dilatation of apex of crypts, petal-like swelling, dilatation of glandular crypts and depletion of goblet cells were visible. Extensively damaged colonic mucosal surface and complete subversion of its architecture were observed. (c, f) SASP group mice: integrity of mucosa architecture, with filamentous microvilli, surface loosening and no swelling.

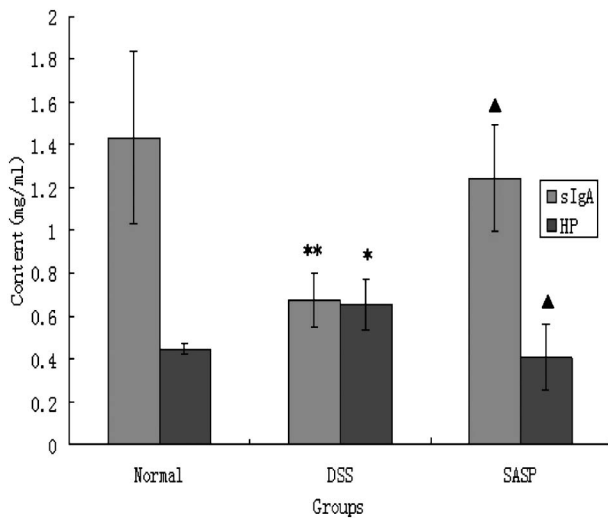


Fig. 6. The Content of sIgA and HP

Data are expressed as mean  $\pm$  S.D. \*\* $p < 0.01$  vs. normal; \* $p < 0.05$  vs. normal; ▲ $p < 0.05$  vs. DSS control.

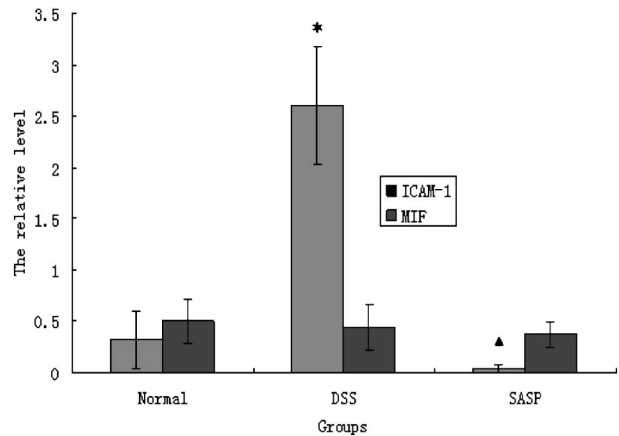


Fig. 7. Examination of ICAM-1 and MIF Genes with SYBR Green I Real-time PCR

GAPDH was used as internal control. DSS activated ICAM-1 gene expression. There was no apparent change of MIF gene expression for SASP. Data are expressed as mean  $\pm$  S.D. \* $p < 0.05$  vs. normal; ▲ $p < 0.05$  vs. DSS control.

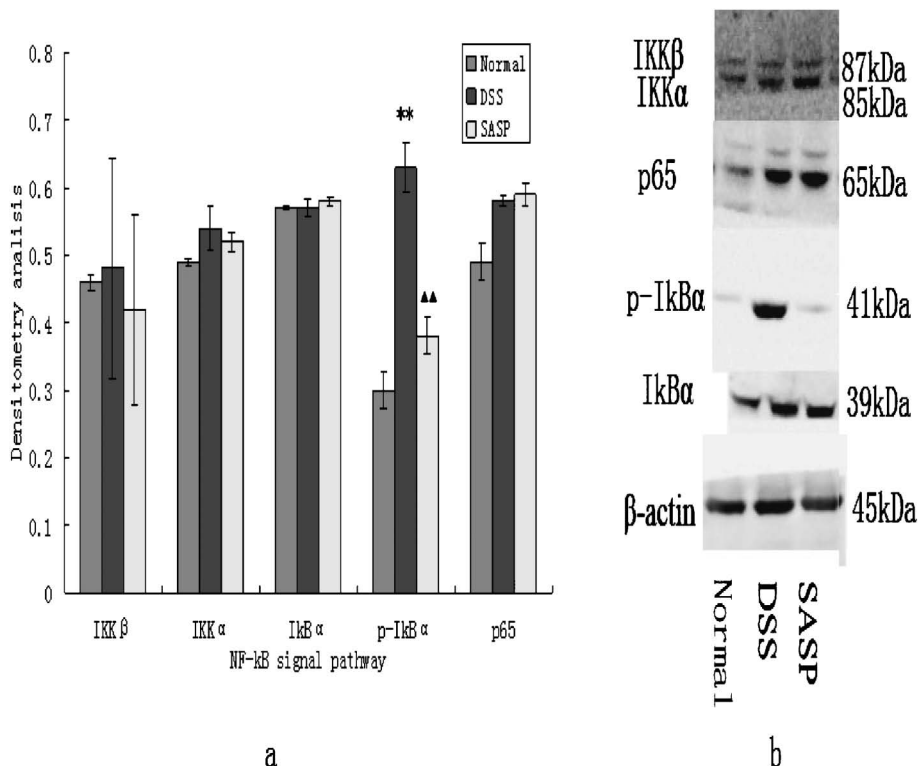


Fig. 8. Expression of IKK $\alpha$ , IKK $\beta$ , p-I $\kappa$ B $\alpha$ , I $\kappa$ B $\alpha$  and p65 as Detected by Western Blotting Analysis  
Chronic administration of DSS induced upregulation of p-I $\kappa$ B $\alpha$  and p65 vs. sham control. SASP inhibited I $\kappa$ B $\alpha$  phosphorylation. Results representative of three independent experiments. Data are expressed as mean  $\pm$  S.D. \*\* $p$  < 0.01 vs. normal; ▲▲ $p$  < 0.01 vs. DSS control.

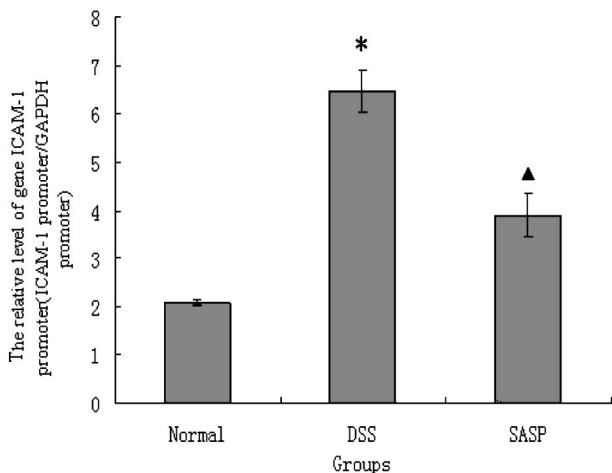


Fig. 9. Relative Level of Gene ICAM-1 Promoter  
DSS activated NF- $\kappa$ B p65 recruitment to ICAM-1 gene promoter in 4 cycles DSS-treated mice, whereas in contrast, SASP reduced NF- $\kappa$ B p65 binding at the ICAM-1 gene promoter. Data are expressed as mean  $\pm$  S.D. \* $p$  < 0.05 vs. normal; ▲ $p$  < 0.05 vs. DSS control.

pathway is the main target of SASP for anti-inflammatory treatment of IBD.

**Acknowledgments** This work was funded by Guangzhou Science and Technology Committee

Grants for significant projects and Guangdong traditional Chinese medicine administration. We thank Dr. Fanqin for molecular biology analyses.

**REFERENCES**

- 1) Rust C., Bauchmuller K., Bernt C., Vennegeerts T., Fickert P., Fuchsbichler A., Beuers U., *Gut*, **55**, 719–727 (2006).
- 2) Cohen H. D., Das K. M., *J. Clin. Gastroenterol.*, **40**, S150–S154 (2006).
- 3) Bergman R., Parkes M., *Aliment. Pharmacol. Ther.*, **23**, 841–855 (2006).
- 4) Karagozian R., Burakoff R., *Ther. Clin. Risk Manag.*, **3**(5), 893–903 (2007).
- 5) Podolsky D. K., *N. Engl. J. Med.*, **347**(6), 417–430 (2005).
- 6) Bouma G., Strober W., *Nature*, **3**, 521–534 (2003).
- 7) Xavier R. J., Podolsky D. K., *Nature*, **448**, 427–435 (2007).
- 8) Visekruna A., Joeris T., Seidel D., Kroesen A., Loddenkemper C., Zeitz M., Kaufmann S. H., Schmidt-Ullrich R., Steinhoff U., *J. Clin. Invest.*, **116**(12), 3195–3203 (2006).

- 9) Morand E. F., *Int. Med. J.*, **35**, 419–426 (2005).
- 10) Van Assche G., Rutgeerts P., *Am. J. Physiol. Gastrointest. Liver Physiol.*, **288**, G169–G174 (2005).
- 11) Park G. Y., Wang X., Hu N., Pedchenko T. V., Blackwell T. S., Christman J. W., *J. Biol. Chem.*, **281**(27), 18684–18690 (2006).
- 12) Hirotani Y., Mikajiri K., Ikeda K., Myotoku M., Kurokawa N., *Yakugaku Zasshi*, **128**(9), 1347–1353 (2008).
- 13) Melgar S., Karlsson A., Michaëlsson E., *Am. J. Physiol. Gastrointest. Liver Physiol.*, **288**(6), G1328–G1338 (2005).
- 14) Shteingart S., Rapoport M., Grodzovski I., Sabag O., Lichtenstein M., Eavri R., Lorberboum-Galski H., *Gut*, **58**(6), 790–798 (2008).
- 15) Borm M. E. A., Bouma G., *Drug Discov. Today Dis. Models*, **1**(4), 437–444 (2004).
- 16) Matos L. L., Stabenow E., Tavares M. R., Ferraz A. R., Capelozzi V. L., Pinhal M. A., *Clinics*, **61**(5), 417–424 (2006).
- 17) Abraham C., Cho J. H., *N. Engl. J. Med.*, **357**, 708–710 (2007).
- 18) Mora J. R., Iwata M., Eksteen B., Song S. Y., Junt T., Senman B., Otipoby K. L., Yokota A., Takeuchi H., Ricciardi-Castagnoli P., Rajewsky K., Adams D. H., von Andrian U. H., *Science*, **314**, 1157–1160 (2006).
- 19) van der Steen L., Tuk C. W., Bakema J. E., Kooij G., Reijerkerk A., Vidarsson G., Bouma G., Kraal G., de Vries H. E., Beelen R. H., van Egmond M., *Gastroenterology*, **137**(6), 2018–2029 (2009).
- 20) Barton G. M., Medzhitov R., *Science*, **300**, 1524–1526 (2003).
- 21) Shimada S., Aoyama T., Shibuya F., Nakajima K., Kotaki H., Sawada Y., Iga T., *Yakugaku Zasshi*, **118**(6), 216–225 (1998).
- 22) Atreya I., Atreya R., Neurath F., *J. Intern. Med.*, **263**, 591–596 (2008).
- 23) de Jong Y. P., Abadia-Molina A. C., Satoskar A. R., Clarke K., Rietdijk S. T., Faubion W. A., Mizoguchi E., Metz C. N., Alsahli M., ten Hove T., Keates A. C., Lubetsky J. B., Farrell R. J., Michetti P., van Deventer S. J., Lolis E., David J. R., Bhan A. K., Terhorst C., *Nat. Immunol.*, **2**(11), 1061–1066 (2001).
- 24) Roebuck K. A., Finnegan A., *J. Leuk. Biol.*, **66**, 876–889 (1999).
- 25) MacDonald T. T., Monteleone G., *Science*, **307** (5717), 1920–1925 (2005).